Article DOI: https://doi.org/10.3201/eid3212.261101

EID cannot ensure accessibility for supplementary materials supplied by authors. Readers who have difficulty accessing supplementary content should contact the authors for assistance.

Natural *Trichuris trichiura* Infections in Endemic Hydromyini Rodents, Papua New Guinea, 2019–2023

Appendix 1

Field sampling and host identification

We investigated whipworm infections in rodents and marsupials sampled at 19 localities in Papua New Guinea, including two elevational transects on Mount Wilhelm (Central Highlands, sampled in 2019) and in the Saruwaged Range (Huon Peninsula, sampled in 2020 and 2023), together with three additional lowland localities (Wanang, Baitabag, and Nagada; Appendix 1 Figure 1). In each mountain system, sampling comprised eight localities spaced at 500 m elevational intervals, ranging from lowland rainforest at 200 m asl to subalpine grassland at 3700 m asl.

Rodents in New Guinea belong to the subfamily Murinae and comprise two major evolutionary lineages: the tribe Rattini, which includes both endemic and introduced *Rattus* species, and the tribe Hydromyini, an endemic Australo–Papuan radiation encompassing ecologically diverse rodents (*1*,*2*). Animals were captured using multiple trap types across major habitat types, including within dwellings; additional specimens were obtained during nocturnal hunts with local Indigenous communities (Appendix Table 1). Sampling procedures are described in Vejmělka et al. (2025) (*2*). Animals were humanely euthanized and measured; host tissues were preserved in ethanol and RNAlater, and gastrointestinal tracts were fixed in ethanol. Host identification was based on morphology and confirmed by sequencing mitochondrial *cytochrome b* or *cytochrome c* oxidase subunit I (*2*). Research in Papua New Guinea was

approved by the National Research Institute and the relevant Provincial Government as the basis for research visa no. 99902702887.

Parasite recovery

The cecum and colon were examined under a stereomicroscope. Whipworms embedded in the intestinal mucosa were carefully removed to preserve specimen integrity. Specimens used for morphometric analysis were cleared in lactophenol and examined as wet mounts. For molecular analyses, the anterior portion of each worm was excised before clearing.

Molecular methods

Genomic DNA was extracted from the anterior portion of each whipworm specimen using the innuPREP Forensic Kit (IST Innuscreen GmbH). Sequencing libraries were prepared using the KAPA HyperPrep Kit (Roche), pooled equimolarly, and sequenced on an Element Biosciences AVITI platform (2 × 300 bp paired-end reads) at the CEITEC Genomics Core Facility (Brno, Czech Republic). Sample cross-talk during multiplexed sequencing was minimized using unique dual indexing, with both i5 and i7 index sequences unique to each library. Reads were assigned to a sample only when both indices matched the expected index pair. Appendix 1 Table 1 provides a sequencing summary and GenBank accession numbers for the sequenced whipworms.

Mitochondrial genome assembly and ITS2 rDNA sequence reconstruction

De novo assembly of mitochondrial genomes was performed with metaSPAdes (*3*). Mitochondrial contigs were identified with BlobTools v1.1.1 (*4*) based on similarity searches against the NCBI and UniProt databases. In all but one sample (NM227), the mitochondrial genome assembled as a single contig; sample NM227 assembled into three contigs. Assemblies were curated in Geneious Prime version 2026.0.2 (https://www.geneious.com): original reads were mapped back to the mitochondrial assemblies and consensus sequences were called using an 85% threshold; contigs of sample NM227 were scaffolded using iterative mapping; and genome orientation was standardized with *cox1* as the starting gene. Assemblies consistently fragmented at the AT-rich region, where read coverage was low or absent; therefore, a stretch of

100 ambiguous nucleotides (Ns) was inserted at this position in each genome. Genomes were annotated by comparison with reference *Trichuris* mitochondrial genomes (GenBank accession nos. NC_028621, MZ229685, KT449826). Sequence similarity of newly assembled genomes was assessed using BLASTN (*5*) against the NCBI nucleotide database to confirm taxonomic identity and identify closely related taxa. Pairwise mitochondrial nucleotide divergence was calculated in MEGA12 (*6*,*7*) for 13 selected *Trichuris* sequences using pairwise deletion of ambiguous positions; the alignment used for this analysis comprised 14,530 bp (Appendix 1 Table 2).

The nuclear ITS2 rDNA marker was reconstructed because it is widely represented in public databases for whipworms and has been shown to discriminate effectively among *Trichuris* species infecting humans (*8*). The ITS2 region was reconstructed using five rounds of low-sensitivity iterative mapping in Geneious Mapper, with the 5.8S rRNA sequence of *Trichuris muris* (GenBank accession FN543136) used as the seed. Consensus sequences were called using a 65% threshold. The same procedure was applied to six representative human-derived *T. trichiura* samples from Doyle et al. (2022) (*9*). In addition, the ITS2 sequence was extracted from scaffold chr2_scaffold39 of the genome assembly of the recently described species *Trichuris incognita* (*10*).

Phylogenetic analyses

Mitochondrial genomes and ITS2 sequences were aligned with representative *Trichuris* sequences from public databases using MAFFT v7.490 (*11*), and ambiguously aligned regions were removed using BMGE (*12*). The final mitochondrial and ITS2 alignments comprised 13,949 bp and 470 bp, respectively. Maximum-likelihood phylogenetic inference was performed in IQ-TREE v3.0.1 (*13*). The TVM+F+I+R3 and TPM3u+F+G4 substitution models, selected by ModelFinder (*14*) (-m MFP) using the Bayesian Information Criterion, were used for the mitochondrial and ITS2 datasets, respectively. Branch support was assessed with 1,000 ultrafast bootstrap replicates (-bb 1000) (*15*) and 1,000 SH-like approximate likelihood ratio test replicates (-alrt 1000) (*16*). *Trichinella spiralis* was used as the outgroup for the mitochondrial dataset. Because ITS2 sequences from *T. spiralis* could not be aligned reliably, the ITS2

phylogeny was midpoint-rooted. Trees were visualized in FigTree v1.4.4 (https://github.com/rambaut/figtree/releases).

References

1. Rowe KC, Achmadi AS, Fabre PH, Schenk JJ, Steppan SJ, Esselstyn JA. Oceanic islands of Wallacea as a source for dispersal and diversification of murine rodents. J Biogeogr. 2019;46:2752–68. https://doi.org/10.1111/jbi.13720

2. Vejmělka F, Fabre PH, Lövy M, Sam K, Helgen KM, Macek M, et al. Complete rainforest elevational gradient reveals unusual diversity patterns of non-volant mammals in New Guinea. Divers Distrib. 2025;31:e70127. https://doi.org/10.1111/ddi.70127

3. Nurk S, Meleshko D, Korobeynikov A, Pevzner PA. metaSPAdes: a new versatile metagenomic assembler. Genome Res. 2017;27:824–34. PubMed https://doi.org/10.1101/gr.213959.116

4. Laetsch DR, Blaxter ML. BlobTools: Interrogation of genome assemblies. F1000 Res. 2017;6:1287. https://doi.org/10.12688/f1000research.12232.1

5. Zhang Z, Schwartz S, Wagner L, Miller W. A greedy algorithm for aligning DNA sequences. J Comput Biol. 2000;7:203–14. PubMed https://doi.org/10.1089/10665270050081478

6. Stecher G, Suleski M, Tao Q, Tamura K, Kumar S. MEGA 12.1: cross-platform release for macOS and Linux operating systems. J Mol Evol. 2026;94:14–8. PubMed https://doi.org/10.1007/s00239-025-10287-z

7. Stecher G, Tamura K, Kumar S. Molecular Evolutionary Genetics Analysis (MEGA) for macOS. Mol Biol Evol. 2020;37:1237–9. PubMed https://doi.org/10.1093/molbev/msz312

8. Rahman N, Bär MA, Dommann J, Hürlimann E, Coulibaly JT, Ali S, et al. Widespread *Trichuris incognita* reveals hidden diversity and reshapes understanding of human whipworm infections. Nat Commun. 2025;16:9831. PubMed https://doi.org/10.1038/s41467-025-64516-6

9. Doyle SR, Søe MJ, Nejsum P, Betson M, Cooper PJ, Peng L, et al. Population genomics of ancient and modern *Trichuris trichiura*. Nat Commun. 2022;13:3888. PubMed https://doi.org/10.1038/s41467-022-31487-x

10. Bär MA, Kouamé NA, Touré S, Coulibaly JT, Schneeberger PHH, Keiser J. Characterisation of *Trichuris incognita* n sp in Côte d'Ivoire: a morphological, genomic, and genome-wide association with drug sensitivity study. Lancet Microbe. 2026;7:101264. PubMed https://doi.org/10.1016/j.lanmic.2025.101264

11. Katoh K, Standley DM. MAFFT multiple sequence alignment software version 7: improvements in performance and usability. Mol Biol Evol. 2013;30:772–80. PubMed https://doi.org/10.1093/molbev/mst010

12. Criscuolo A, Gribaldo S. BMGE (Block Mapping and Gathering with Entropy): a new software for selection of phylogenetic informative regions from multiple sequence alignments. BMC Evol Biol. 2010;10:210. PubMed https://doi.org/10.1186/1471-2148-10-210

13. Wong TKF, Ly-Trong N, Ren H, Demotte P, Baños H, Roger AJ, et al. IQ-TREE 3: phylogenomic inference software using complex evolutionary models. Mol Biol Evol. 2026;43:msag117. PubMed https://doi.org/10.1093/molbev/msag117

14. Kalyaanamoorthy S, Minh BQ, Wong TKF, von Haeseler A, Jermiin LS. ModelFinder: fast model selection for accurate phylogenetic estimates. Nat Methods. 2017;14:587–9. PubMed https://doi.org/10.1038/nmeth.4285

15. Hoang DT, Chernomor O, von Haeseler A, Minh BQ, Vinh LS. UFBoot2: improving the ultrafast bootstrap approximation. Mol Biol Evol. 2018;35:518–22. PubMed https://doi.org/10.1093/molbev/msx281

16. Anisimova M, Gil M, Dufayard JF, Dessimoz C, Gascuel O. Survey of branch support methods demonstrates accuracy, power, and robustness of fast likelihood-based approximation schemes. Syst Biol. 2011;60:685–99. PubMed https://doi.org/10.1093/sysbio/syr041

Appendix 1 Table 1. Sequencing summary for whipworm specimens included in the genetic analyses, Papua New Guinea, 2019–2023.

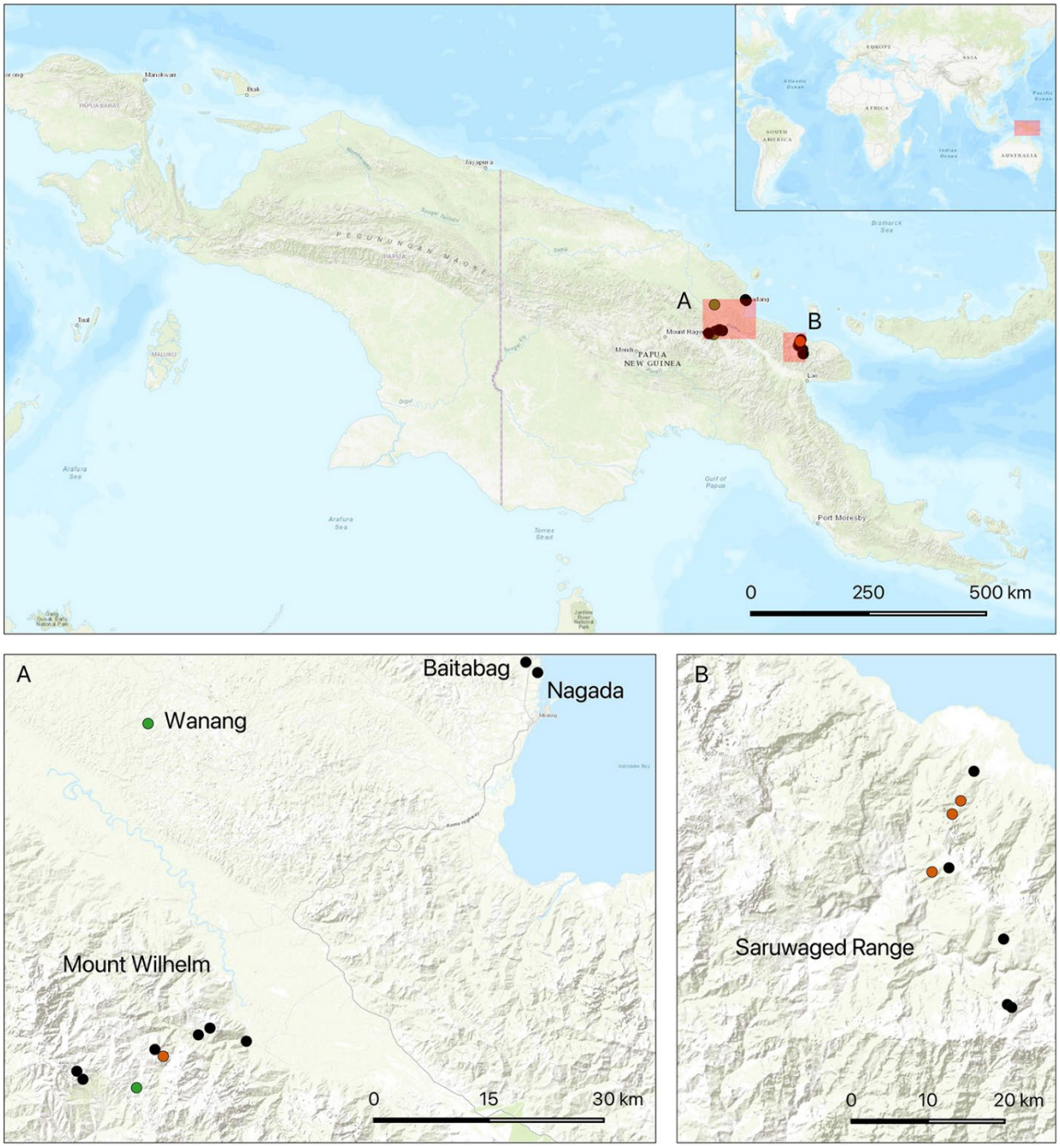
					ITS2			mtDNA		
Sample ID	Host ID	Host species	GenBank accession no.	Total reads	GenBank accession no.	No. mapped reads	Coverage, mean ±SD	GenBank accession no.	No. mapped reads	Coverage, mean ±SD
NM222	FR1700.082	*Hyomys goliath*	PZ184053	1,741,004	PZ173638	4,661	1,797 ± 145	PZ188518	56,110	1,180 ± 259
NM223	FR1700.001	*Mallomys hercules*	NA	4,563,814	PZ173639	8,231	3,063 ± 391	PZ188519	85,544	1,790 ± 311
NM224	FR700.004	*Pogonomys macrourus*	PZ184054	1,815,668	PZ173640	3,214	1,227 ± 110	PZ188520	134,596	2,827 ± 427
NM225	FR700.021	*Uromys caudimaculatus*	PZ184055	3,070,294	PZ173641	7,553	2,800 ± 366	PZ188521	40,951	854 ± 168
NM226	FR1200.035	*Mallomys hercules*	PZ184056	3,397,134	PZ173642	4,015	1,443 ± 230	PZ188522	31,980	666 ± 119
NM227	WG200.001	*Hydromys chrysogaster*	PZ184057	3,295,432	PZ173643	6,340	2,883 ± 122	PZ188523	25,208	520 ± 97
NM228	FR1700.003	*Uromys* sp. 1	PZ184058	838,162	PZ173644	2,768	1,044 ± 97	PZ188524	2,074	40 ± 12
NM232	MW1700.100	*Pogonomys loriae*	PZ184059	3,388,044	PZ173645	4,751	1,713 ± 270	PZ188525	77,503	1,611 ± 258
NM233	MW1700.033	*Pogonomys loriae*	PZ184060	985,170	PZ173646	1,162	405 ± 77	PZ188526	44,428	847 ± 162
NM234	MW2700.041	*Rattus niobe*	PZ184061	877,682	PZ173647	407	205 ± 8	PZ188527	2,500	48 ± 12
NM235	MW2700.098	*Rattus niobe*	PZ184062	2,579,878	PZ173648	2,480	1,233 ± 63	PZ188528	235,736	4,903 ± 857

*ITS2, internal transcribed spacer 2 ribosomal DNA; mtDNA, mitochondrial DNA; NA, not available; SD, standard deviation. Coverage values are mean±SD. Vermilion indicates *Trichuris trichiura*; green indicates rodent-associated *Trichuris* spp.

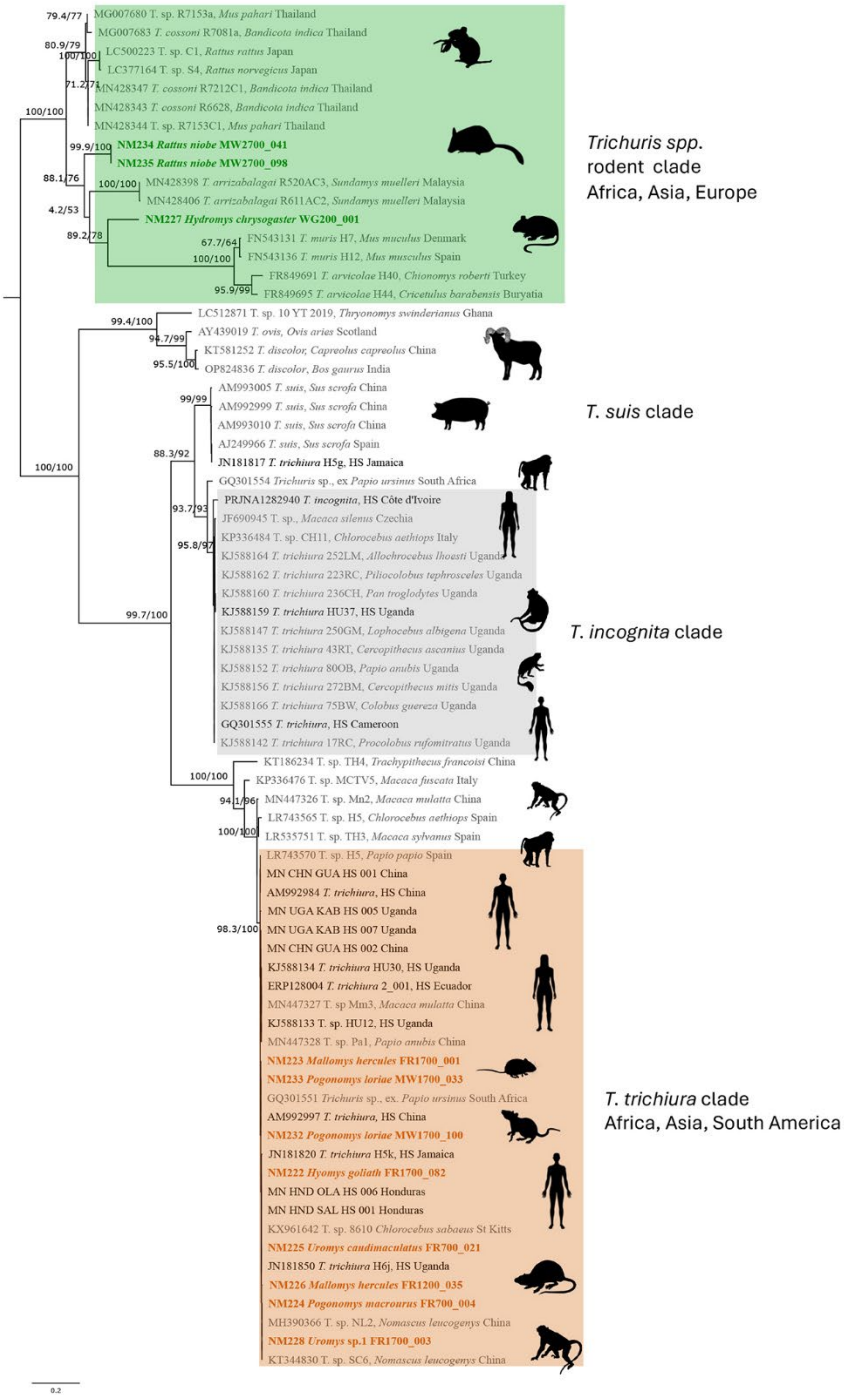
Appendix 1 Table 2. Pairwise mitochondrial nucleotide divergence among *Trichuris* specimens from wild rodents in Papua New Guinea, 2019–2023, and selected human-derived *Trichuris trichiura* reference sequences*

Sequence	NM222	NM223	NM225	NM228	NM232	NM233	NM224	NM226	AP017704	HND003	NM227	NM234	NM235
NM222	—												
NM223	0.70	—											
NM225	0.89	0.97	—										
NM228	0.85	0.92	0.27	—									
NM232	0.99	1.05	0.87	0.83	—								
NM233	1.16	1.20	1.03	0.99	1.05	—							
NM224	1.69	1.69	1.55	1.52	1.62	1.69	—						
NM226	1.66	1.70	1.56	1.53	1.64	1.71	0.63	—					
AP017704	2.42	2.50	2.32	2.30	2.36	2.43	2.27	2.30	—				
HND003	2.44	2.52	2.33	2.32	2.37	2.45	2.30	2.32	0.06	—			
NM227	34.12	33.98	34.04	33.99	33.98	33.96	33.95	33.91	33.89	33.92	—		
NM234	33.85	33.95	33.92	33.85	33.82	33.89	33.82	33.79	33.75	33.74	18.55	—	
NM235	33.85	33.95	33.92	33.85	33.82	33.89	33.82	33.79	33.75	33.74	18.56	0.00	—

*Values are pairwise nucleotide divergence (%), calculated as the number of base differences per site × 100. The analysis included 13 mitochondrial sequences and 14,530 aligned nucleotide positions. Ambiguous positions were removed for each sequence pair using pairwise deletion. Analyses were conducted in MEGA12.
NM222, *Hyomys goliath*, FR1700.082; NM223, *Mallomys hercules*, FR1700.001; NM225, *Uromys caudimaculatus*, FR700.021; NM228, *Uromys* sp. 1, FR1700.003; NM232, *Pogonomys loriae*, MW1700.100; NM233, *P. loriae*, MW1700.033; NM224, *Pogonomys macrourus*, FR700.004; NM226, *Mallomys hercules*, FR1200.035; NM227, *Hydromys chrysogaster*, WG200.001; NM234, *Rattus niobe*, MW2700.041; NM235, *R. niobe*, MW2700.098. AP017704, human-derived *T. trichiura* reference sequence from Ecuador; HND003, human-derived *T. trichiura* sequence MN_HND_OLA_HS_003 from Honduras.

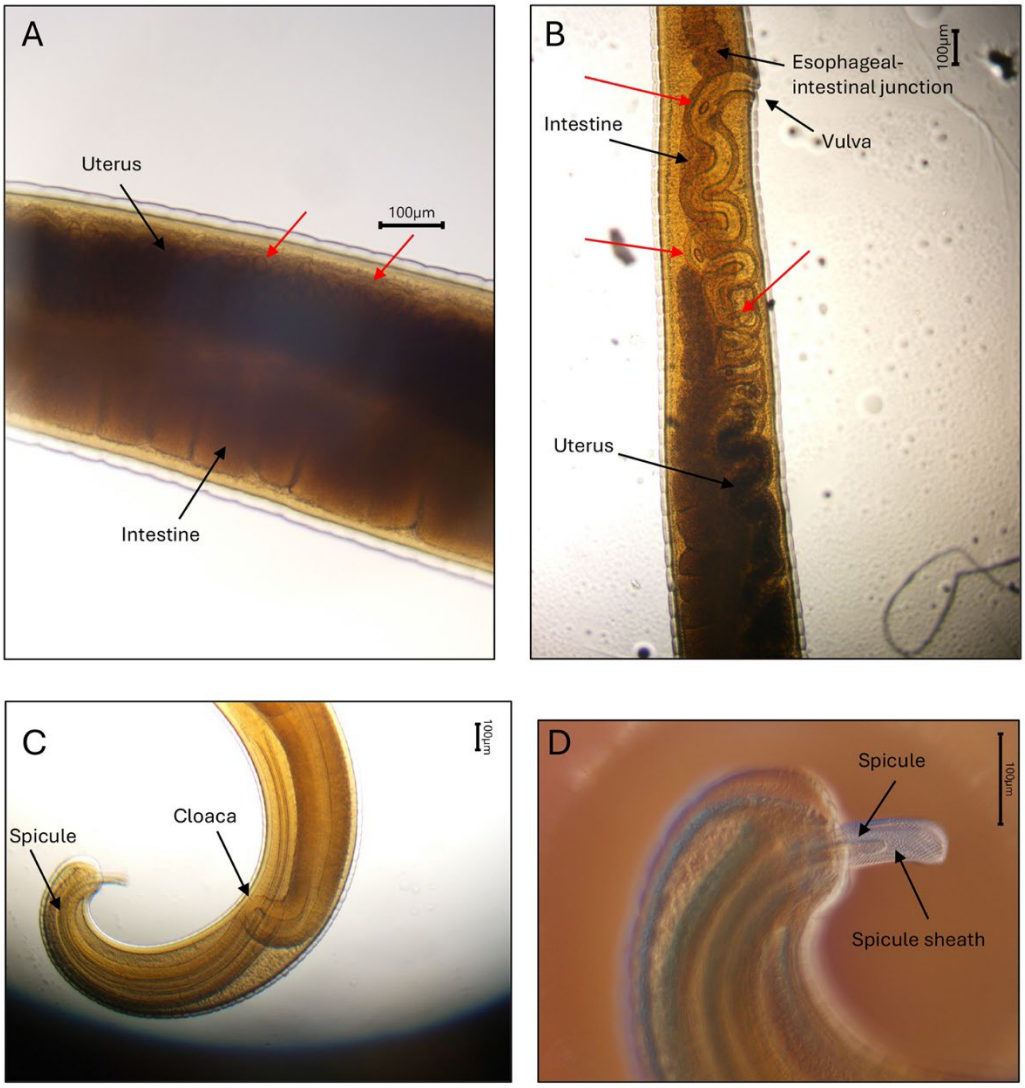


Appendix 1 Figure 1. Sampling localities and distribution of *Trichuris* infections in wild mammals, Papua New Guinea, 2019–2023. (A) Mount Wilhelm and the lowland sites of Wanang, Nagada, and Baitabag. (B) Saruwaged Range sampling sites. Black circles indicate sampled localities; vermilion circles, sites where *Trichuris trichiura* was detected; green circles, sites where rodent-associated *Trichuris* spp. were detected. Maps were created in QGIS v3.30 using the Esri World Topographic Map as a basemap.



Appendix 1 Figure 2. Maximum-likelihood phylogeny of the genus *Trichuris* based on ITS2-rDNA sequences from wild rodents in Papua New Guinea, 2019–2023, and publicly available sequences representative of the genus. Sequences generated in this study are shown in bold. Vermilion indicates *Trichuris trichiura*; green indicates rodent-associated *Trichuris* spp. Tip labels show database accession number, host species, and country of origin. Human-derived reference sequences (HS) are shown in black; all other reference sequences are shown in gray. The tree is midpoint-rooted. Node labels show

SH-aLRT (%) and ultrafast bootstrap (%) branch support. The scale bar indicates substitutions per site. Sequences belonging to the recently described *T. incognita* clade were originally deposited in GenBank as *T. trichiura*; original sequence names were retained for consistency with public records. Animal silhouettes are from PhyloPic (CC0 1.0).



Appendix 1 Figure 3. Morphology of *Trichuris trichiura* recovered from *Mallomys hercules* (FR1700_001), Saruwaged Range, Papua New Guinea, 2023. A total of 122 whipworms were recovered from this host. (A) Portion of the uterus of an adult female containing numerous developed eggs (red arrows) (100× magnification). (B) Female at the esophageal–intestinal junction, showing the vulva, intestine, uterus, and developed eggs in the vagina (red arrows) (5× magnification). (C) Posterior end of an adult male showing the spicule and cloaca (50× magnification). (D) Detail of the posterior end of an adult male showing the spicule and spicule sheath (200× magnification).